AQUEOUS HYDROGEN PEROXIDE-INDUCED DEGRADATION OF POLYOLEFINS: A GREENER PROCESS FOR CONTROLLED-RHEOLOGY POLYPROPYLENE

Graeme Moad[a, b], Ian J.Dagley[a], Jana Habsuda[a, c], Christopher J. Garvey[a, d], Guoxin Li[a, b], Lance Nichols[a, b], George P. Simon[a, c], Maria Rossella Nobile[e]

[a] CRC for Polymers, 8 Redwood Drive, Notting Hill, Victoria 3168, Australia
[b] CSIRO Manufacturing, Bayview Ave, Clayton, Victoria 3168, Australia
[c] Monash University, Department of Materials Engineering, Clayton, Victoria 3800, Australia
[d] Bragg Institute, Australian Nuclear Science and Technology Organisation, Lucas Heights, NSW 2234, Australia
[e] University of Salerno, Department of Industrial Engineering, 84084 Fisciano, Salerno, Italy

Abstract
In this work we demonstrate that aqueous hydrogen peroxide is an effective reagent for chain scissioning or vis-breaking of polypropylene during melt-processing to produce a controlled rheology product. The novel process involves the direct injection of aqueous hydrogen peroxide into the polypropylene melt under pressure. The polypropylene produced has reduced molar mass, narrowed molar mass distribution, and is indistinguishable in terms of melt flow rate, molar mass distribution, crystallinity and melt rheology from conventionally vis-broken polypropylene produced using an organic peroxide (2,5-dimethyl-2,5-di-tert-butylperoxyhexane (DHBP)). However, the polypropylene produced in the current process is notably free of the initiator-derived organic volatiles that are formed as by-products in the case where organic peroxides such as DHBP are used.

1. Introduction
Ex-reactor conventionally-formed polypropylene is characterized by a broad molar mass distribution (MMD). So called "controlled rheology" grades of lower molar mass and dispersity are produced in a subsequent in-line melt processing step in an extruder. These grades possess improved processability and the specific rheological behaviour required for many applications which include fibre and thin-wall injection-moulding [1-4]. The process has been described fully in reviews describing reactive extrusion processing of polyolefins [1-4] and usually involves radical-induced chain-scissioning or vis-breaking. The reagents most commonly used as a source of radicals are organic peroxides [4], which include cumyl peroxide [5-11], di-tert-butyl peroxide [12], 2,5-dimethyl-2,5-di-tert-butylperoxyhexane (DHBP; also known under trade names such as Luperox™ 101 or Triganox™ 101) [10, 13-25], di(tert-butylperoxyisopropyl)benzene [26] and other peroxides [24]. However, the use of these organic peroxides in this context suffers from a number of drawbacks, most notably, the formation of organic volatiles, such as tert-butanol and acetone in the case of DHBP (Scheme 1) [4]. This has provided the impetus for a significant effort in developing other initiators for use in the process. These include cyclic peroxides [27] and a range of non-peroxide initiators, which include certain azoalkanes [28] and alkoxyamines [29-31], and UV photoinitiators [32].

Scheme 1

Hydrogen peroxide is sometimes mentioned in lists of suitable initiators in various patents and is mentioned in at least one book [33] as an initiator used in forming controlled rheology polypropylene, though to our knowledge there are no actual examples of such use [1-4]. Given the inherent incompatibility of water and polyolefin-melts, it seems counterintuitive to contemplate the direct use of an aqueous peroxide solution in melt-extrusion of polypropylene at high temperatures. Nonetheless, there is an obvious advantage to the use of hydrogen peroxide in the context of vis-

breaking, in that the only expected initiator-derived by-product is water. Our initial research on the use of aqueous hydrogen peroxide in vis-breaking is described in a recent patent application [34].

The mechanism of vis-breaking using organic peroxides is usually described as shown in Scheme 2 [35]. The process involves formation of tertiary radicals (α to the polypropylene methyl) on the backbone that undergo β-scission to form a polypropylene propagating radical and an unsaturated chain end. Bertin et al. [36-37] have suggested a very different mechanism. They explored polypropylene degradation in solution at 140–165 °C and surprisingly found for experiments under inert atmosphere that there was a small increase in molar mass. It should be noted that the conditions used in the present study, and in the industrial process for producing controlled rheology polypropylene (~280 °C, polymer melt), differ markedly from those used by Bertin et al. [37] (140–165 °C, solution). They [37] found that efficient chain-scissioning required the presence of oxygen. They also proposed on the basis of density functional calculations that, contrary to expectations based on relative bond strengths, hydrogen abstraction by tert-butoxy (and other tert-alkoxy radicals) radical should occur preferentially from the polypropylene methyls due to a more favourable entropy of activation. The primary radicals so formed do not readily undergo β-scission and terminate mainly by combination. They [37] speculated that the efficiency of chain scission observed in the commercial vis-breaking process was therefore dependent on the presence of oxygen and the formation of methylperoxy and hydroxy radicals, which they proposed should show less selectivity.

Scheme 2

These proposals [37] are not supported by more recent theoretical and experimental work. Gryn'ova et al. [38] found using high level ab initio calculations that the reactions of peroxyl radicals with unactivated hydrogens is extremely endothermic such that they unfavourable even at elevated temperatures and are unlikely to be involved in oxidative degradation. Other studies have found that oxidative degradation provides a polypropylene containing various functionality at the chain ends and along the backbone which are observable using such techniques as FTIR spectroscopy and CRYSTAF [39].

Garrett et al. [11] used radical trapping to examine the regioselectivity of hydrogen abstraction from model substrates by cumyloxy radicals at 160 °C. They found that, while steric factors reduced the rate of abstraction or methine and methylene hydrogens, the methine hydrogens of 2,4-dimethylpentane were nonetheless abstracted preferentially (Fig. 1). Similar observations were made by Dokolas et al. [40] for hydrogen abstraction from 2,4-dimethylpentane by tert-butoxy radicals at 60 °C (Fig. 1). These data appear in general agreement with reactivities estimated in EPR studies by Camara et al. [41].

Fig. 1

The process with hydrogen peroxide is anticipated to produce hydroxy radicals thermally or by induced decomposition [42-43]. Hydroperoxy radicals can also be formed by hydrogen-atom abstraction from hydrogen peroxide [42]. It is also possible to form oxygen from hydrogen peroxide. We have found in previous work that oxygen will cause scissioning of polypropylene, though the product formed is discoloured and there is some formation of volatile byproducts. We also found that the process is catalysed by transition metals such as copper [44].

In this work we describe the process condition for vis-breaking polypropylene with hydrogen peroxides in melt extrusion. We characterize the polymer by molar mass, MMD, crystallinity and dynamic rheological properties and compare properties with those for the similar polymer formed by vis-breaking with DHBP.

2. Experimental

2.1. Materials

The polypropylene grades (HP400N, HP555G) used are manufactured by Lyondell-Basell and contain a proprietary stabilizer package. Aqueous hydrogen peroxide (59.5% w/w) Interox®ST-60 was obtained from Solvay Interox Pty Ltd Australia. DHBP was obtained from United Initiators Gmbh.

2.2. Extrusion

All extrusion experiments were carried out with a JSW TEC30 twin screw extruder with L/D 47. A flat temperature profile was used where zone 2 was set to 160 °C. Zones C3–C14 (of 14) were all set to 280 °C and the die was set to 220 °C. Polypropylene was added to the nitrogen blanketed hopper through a Brabender Flexiwall FW40/5-50 gravimetric feeder at 20 kg h^{-1}. Aqueous hydrogen peroxide was injected under pressure into the propylene melt stream at C4 using a Teldyne-Isco 500D syringe pump through a cooled injection nozzle. On exit of the die, the strand was cooled by passage through an ambient temperature water bath (2.4 m × 300 mm × 300 mm), pelletized, collected and dried at ambient temperature (typically ∼24 °C). Full details of the screw configuration and temperature profile are shown in the Supplementary material.

2.3. Melt flow rate (MFR) measurements

Melt flow rate (MFR) measurements were performed according to ASTM D1238 [45] (230 °C/2.16 kg for polypropylene). The units for MFR are g/10 min using an IDM instruments melt flow indexer.

2.4. Size exclusion chromatography (SEC)

Size exclusion chromatography (SEC) or gel permeation chromatography was performed with a GPC PL 220 from Polymer Laboratories (Agilent) instrument equipped with a refractive index detector and two linear Olexis columns (each 300 × 8 mm) from Polymer Laboratories. The mobile phase was 1,2,4-trichlorobenzene which was purified by vacuum distillation and stabilized with 3,5-di-tert-4-butylhydroxytoluene (BHT, 200 mg L^{-1}). The injection system, columns and detector were maintained at 150 °C. The sample concentration was 1 mg mL^{-1}.

2.5. Crystallization analysis fractionation (CRYSTAF)

A CRYSTAF model 200 from Polymer Char S.A. (Valencia, Spain) was used for crystallization fractionation. The sample (20 mg) was dissolved in 1,2,4-trichlorobenzene (30 mL). The cooling rate used was 0.1 °C min^{-1} [39].

2.6. Differential scanning calorimetry (DSC)

A Mettler Toledo DSC821e equipped with a TSO 801RO sample robot and ATARe software version 9.00a was used. Experiments were performed under nitrogen (50.0 mL min^{-1}). The temperature program involved heating the sample from 40.0 to 240.0 °C at 10.0 °C min^{-1}, maintaining the sample at 240.0 °C for 10.0 min then cooling from 240.0 to 40.0 °C at −20 °C min^{-1}. The program was then repeated.

2.7. Density

Density of materials at 23.0 °C was measured using an AccuPyc 1330 Pycnometer. The sample (1–1.5 g) each were placed in a cylindrical container (5 mL), which was purged with helium. The purge fill pressure was set to 19.5 psig (134.447 KPa) with an equilibration rate of 0.005 psig min^{-1} (34.47 Pa min^{-1}). The densities reported in Table 1, Table 2 are the average over 10 measurements.

Table 1

Table 2

The crystalline fraction was calculated using the relationship

$$(1-\lambda)_{\mathrm{d}} = ((1/\rho_{\mathrm{a}}) - (1/\rho)) / ((1/\rho_{\mathrm{a}}) - (1/\rho_{\mathrm{c}})) \qquad 1$$

where ρ is the measured density and ρ_a and ρ_c are the densities of completely amorphous and pure crystalline phase; 0.854 g cm^{-3} and 0.936 g cm^{-3} respectively [46].

2.8. Wide angle X-ray scattering (WAXS) (conventional X-ray source)
The measurements were carried out on a Phillips 1130 diffractometer using CuKα radiation (wavelength 0.1542 nm) operated at 40 kV and 25 mA. The scattering angle (2θ) covered the range from 2° to 35° (θ is Bragg angle) with a step of 0.02° at speed 1.0° min^{-1}. The pellets were ground to powder under liquid nitrogen and stored in polyethylene bags at room temperature prior to the experiment. In order to estimate the crystalline fraction, Gaussian functions were used to describe the amorphous and crystalline peaks. The overall crystallinity was then calculated as the ratio of the total of the fitted crystalline areas to fitted total crystalline plus amorphous areas. The procedure has been described in detail by Zhu et al. [47]. A second estimate of the crystalline fraction was provided by the program Traces™ (version 6).

2.9. Small angle and wide angle X-ray scattering (SAXS and WAXS) (synchrotron source)
Samples prepared as above were packed in a 1.5 mm quartz capillary. SAXS and WAXS scattering patterns were simultaneously acquired on the SAXS/WAXS beam line at the Australian Synchrotron. For each sample 2 single measurements of 1 s were averaged from different spots on the capillary. The sample measurements were complemented by a background measurement of 2 by 1 s measurements on an empty capillary in air. There was no difference between duplicate measurements. Further details of methods and data analysis are provided in the Supplementary material.

2.10. Melt rheology
The complex viscosity (η*), the storage (G′) and the loss (G″) moduli were measured using a Rheometrics Scientific ARES (Advanced Rheometric Expansion System), equipped with a 2KFRTN1 transducer, in oscillatory mode. A parallel plate geometry 50 mm in diameter and 1 mm gap was used.

The samples were loaded as extruded pellets and annealed at 240 °C for 10 min prior to commencing the experiments. The linear viscoelastic region of each material was determined at two different temperatures (190 °C and 240 °C), at 10 rad s^{-1} frequency under nitrogen atmosphere after being assessed for thermal stability at the same temperatures and frequency. The frequency scans were performed at a minimum of six different temperatures between 130 °C or 140 °C and 240 °C under nitrogen atmosphere at 10% strain over a frequency range of 0.01–100 rad s^{-1}.

3. Results and discussion
3.1. Processing
Initial experiments on hydrogen-peroxide induced vis breaking are described in our patent application [34]. These experiments explored the manner of addition, the hydrogen peroxide concentration and addition rate, the polypropylene feed rate, the screw design and temperature profile, and the effects of additives and stabilizers.

The experiments described here were designed to establish the dependence of the extent of vis-breaking of polypropylene on the hydrogen peroxide addition rate. All experiments were conducted on a JSW TEC-30 twin screw L/D 47 operating with a 20 kg h^{-1} throughput of polypropylene. Two

grades of commercial polypropylene were used, namely Lyondell-Basell HP400N (nominal MFR 11) and HP555G (nominal MFR 1.5). The aqueous hydrogen peroxide was injected under pressure through a cooled injection nozzle into the polypropylene melt at zone C4, which is beyond the initial melt seal. The MFR changes observed are reported in Fig. 2a. Further details are reported in the Supporting information.

Fig. 2

Even though the extruder was not vented, the extrudate exhibited no foaming for addition levels of aqueous peroxide or water <1000 ppm (volume/volume), and no surface defects for water/peroxide addition rates <600 ppm (i.e. a smooth strand was produced that was indistinguishable in appearance from a strand produced by direct extrusion of polypropylene without addition of water or peroxide).

Samples of the extrudate were collected for determination of organic volatiles and for gel count measurements. As expected, ethanol, acetone and tert-butanol, which are the normal by-products observed in vis-breaking with DHBP, were below the limit of detection. Additionally, there was no elevation of hydrocarbon volatiles, which appeared typical of those observed for polypropylene formed with DHBP using conventional process. Gel count analysis showed that the level of gels was similar to or below those seen with DHBP, and well within normal specifications for controlled rheology polypropylene [34].

In order to evaluate the importance of shear-induced degradation under the process conditions, a series of experiments with HP400N was carried out with addition of equal volume of water rather than aqueous hydrogen peroxide and otherwise similar conditions. No vis-breaking, as would be evidenced by an MFR shift, was observed.

Vis-breaking of polypropylene with aqueous hydrogen peroxide was directly compared the same process using DHBP. When injected into the melt steam at 280 °C under our processing conditions, DHPB was ineffective and resulted in minimal vis-breaking. This is attributed to the residence time of the peroxide in the injection nozzle and its decomposition prior to injection. Accordingly, the DHBP was injected onto the conveyed polypropylene pellets in a manner that emulates the conventional method for organic peroxide addition during the commercial vis-breaking process. It should be noted that when aqueous hydrogen peroxide was added to the polypropylene prior to the initial melt seal in this way, hydrogen peroxide was not effective in vis-breaking. This is attributed to the volatility of hydrogen peroxide and consequent loss of the peroxide through the hopper. Small amounts of hydrogen peroxide were detected using moistened peroxide test strips in these circumstances.

A similar series of extrusion experiments was carried out with DHBP and both HP400N and HP555G. Given the above-mentioned factors, the temperature profile for the experiments with DHBP was modified such that the set temperature over the injection zone was lower (i.e. C2 160, C3 220, C4 170 °C) so as to avoid premature decomposition of the organic peroxide. The results of these experiments are reported in Fig. 2b. After correcting for peroxide concentration, the hydrogen peroxide is ca 20% more effective than DHBP on a weight or volume basis (Fig. 3). However, on a "moles of peroxide" basis, the DHBP (molar mass 294 g mol^{-1}) is substantially more effective than hydrogen peroxide (molar mass 34 g mol^{-1}).

Fig. 3

The finding that the vis-breaking effectiveness with both hydrogen peroxide and DHBP becomes increasingly more effective for higher addition rates can be attributed to the peroxide initially

reacting with the stabilizer package present in the commercial polypropylene. This hypothesis is supported by the observation of significantly higher reaction efficiency when unstabilized reactor powder is used in the process with hydrogen peroxide as initiator [34].

3.2. Size exclusion chromatography (SEC) molar mass distributions

MMD were obtained by size exclusion chromatography (SEC) for HP400N and HP55G and the samples that were vis-broken for a 60% aqueous hydrogen peroxide addition rate of 0.2 mL min^{-1} (~600 ppm volume/weight) or 0.333 mL min^{-1} (~1000 ppm). The data are compared with data for a polypropylene scissioned with 0.165 mL min^{-1} DHBP, which provided a similar MFR as that produced with 0.2 mL min^{-1} of hydrogen peroxide. The molar mass averages in polystyrene equivalents for these samples are reported in Fig. 4 and the MMD are displayed in Fig. 5.

Fig. 4

Fig. 5

As anticipated, the distributions shift from the original position towards lower molar mass for the scissioned samples. The vis-breaking process preferentially cleaves chains of higher molar mass, thereby providing a polymer with a narrower MMD. The molar mass averages and the MMD for polymers of similar MFR formed by vis-breaking with aqueous hydrogen peroxide and DHBP appear similar and the latter are consistent with data in the literature for polymer vis-broken with organic peroxides [12, 24]. While a significant MFR shift shows that the extent of chain scissioning increases with the level of peroxide used, the effect on the molar mass averages and MMD of increasing the hydrogen peroxide addition rate from 0.2 mL min^{-1} to 0.333 mL min^{-1} appears small (within experimental error). The same conclusion follows from the analysis of rheological data (vide infra).

3.3. Rheological properties

The complex viscosity (η*), the storage (G′) and the loss (G″) moduli for the selected samples were measured as a function of temperature (T) and frequency (ω) using a Rheometrics Scientific ARES (Advanced Rheometric Expansion System). The η* values obtained at various temperatures for HP400N and HP555G and for the derived vis-broken samples, were shifted along the frequency axis to obtain the master curves shown in Fig. 6 at the reference temperature (T0) of 190 °C. The time–temperature superposition principle (TTS) [48] was applicable over the entire temperature range and the derived horizontal shift factors (a_T) for the two series are reported in Fig. 7. The temperature dependence of the shift factors can be expressed in terms of an Arrhenius relationship

$$a_{\mathrm{T}} = \exp\left[\frac{E_{\mathrm{a}}}{R}\left(\frac{1}{T} - \frac{1}{T_0}\right)\right] \qquad 2$$

where R is the universal gas constant, Ea is activation energy for flow and T0 is the reference temperature. The calculated Ea for flow at the reference temperature of 190 °C for the HP400N series is 46.0 kJ mol^{-1}. A similar value (46.4 kJ mol^{-1}) was obtained in the case of the HP555G series. These values are consistent with activation energies reported in literature for isotactic polypropylene [49-53]. The low Ea values for isotactic polypropylene indicate that flow properties of polypropylene are not strongly temperature dependent.

Fig. 6

Fig. 7

The temperature window for the rheological measurements of the isotactic polypropylene melts is limited at the low end by the onset of crystallization (melt temperature (Tm) ~ 165 °C) and at the high end >240 °C by degradation. This narrow temperature window, combined with a low temperature coefficient of viscosity, restricts the range of frequencies that can be obtained in the master curves [19, 50-54]. To perform viscoelastic measurements at low temperatures (130 or 140 °C) the polypropylene samples were melt annealed then cooled to the test temperature. The measurement time was set so as to be shorter than the induction time for crystallization suggested by DSC experiments. This maximizes the amount of complex viscosity data obtainable at higher frequencies in the master curves (Fig. 6a and b). The overlap of the data collected at different temperatures was very good for all samples.

The virgin polypropylene samples show shear thinning behaviour at higher frequencies and a tendency for Newtonian behaviour at the lower frequencies. Consistent with their lower molar mass averages, the results (Fig. 6a and b) show that the controlled rheology grades are characterized by viscosity values much lower than the virgin polypropylene samples. A shift toward more Newtonian behaviour is also clearly observed for all the controlled rheology polypropylene samples because of their narrower MMD. Our results show that the flow curves of vis-broken polypropylene obtained with aqueous peroxide and DHBP appear similar. The data are consistent with that reported in the literature for polypropylene vis-broken with DHBP and other organic peroxides [8, 19, 54-56].

The zero shear viscosity η_0 at T = 190 °C of the investigated samples was evaluated from the master curves as the limiting value of the complex viscosity

$$\eta_0 = \lim_{\omega \to 0} \eta^* \qquad 3$$

In the case of the vis-broken polypropylene samples, there is a clear plateau in the viscosity at the lowest frequencies, indicating that the Newtonian region has been reached in the frequency window investigated. In contrast, the limiting region was not observed for the virgin polypropylene. In all the cases, the estimate of η0 was obtained using a fit of the experimental viscosity data to the Carreau–Yasuda model (equation (4)) as shown in Fig. 6a and b [57].

$$\eta = \eta_0 \left[1 + (\lambda\omega)^a\right]^{\frac{n-1}{a}} \qquad 4$$

where η0, λ a and n are the fitting parameters.

The Carreau–Yasuda model zero shear viscosity values as a function of the SEC Mw are reported as a log–log plot in Fig. 8.

Fig. 8

The viscosity η0 data can be correlated with the scaling relation

$$\eta_0 = K\, M_{\mathrm{w}}^{\alpha} \qquad 5$$

where K is a material constant and α is a scaling exponent.

The power–law correlation should hold for linear polymers that contain fractions with molar masses larger than the critical molar mass, Mc (~7000 g mol^{-1} for polypropylene [58]) where entanglements begin to have a significant effect on the chain dynamics. The scaling relation of the η0 data is shown in Fig. 8 as a straight line with a slope of 3.6. The results demonstrate that the η0 values of vis-broken polypropylene with aqueous peroxide and DHBP can be described by the same

power law correlation. Indeed, the viscosity–molar mass power law correlation for many uniform polymers can be described using an exponent α of value 3.4 [48]. In the case of polypropylene values α = 3.6 [49, 53, 59-61], α = 3.5 [51], α = 3.7 [62-63] and α = 3.9 [19] have been reported for the power law exponent for both isotactic and atactic polypropylene. A value of α = 3.4 has been reported for metallocene polypropylene with a relatively low dispersity (Mw/Mn ∼2) [51, 52, 64, 65]. Our results are, therefore, consistent with the literature results. The "Mw rule" for the viscosity–molar mass power law correlation generally can be satisfactorily applied for mildly disperse polymers [66, 67]. However, the relationship begins to break down for higher dispersity polymers. In this latter case, Zeichner and Patel [61] enclosed the (Mw/Mn)0.84 term in the viscosity–molar mass power law correlation, while Wasserman and Graessley [53] preferred to use a Mz/Mw term because it better reflects the breadth of the high molar mass tail of the MMD.

In general, the rheological behaviour of polymer melts strongly depends on their MMD. The increase in the breadth of the MMD of polymers influences the shape of the viscosity vs shear–rate curve, which shows a decrease in the characteristic shear rate for the onset of non-Newtonian behaviour. This is clearly evident from the results reported in Fig. 6 for the virgin polypropylene, which are characterized by a broad MMD, and for the controlled rheology polypropylene melts, which have a narrower MMD. Concerning the linear viscoelastic response, the effects of dispersity are reflected in the broadening of the relaxation spectrum in the plateau and terminal regions. Recently different blending laws have been proposed to describe the mixing effect on the rheological behaviour of linear flexible disperse polymers. Mixing rules have been applied both to the flow curve [68, 69] as well as to the viscoelastic properties of entangled polymer melts [70-77]. Among these, the double-reptation model [72-74, 76] has been successfully applied to describe the effects of MMD in the plateau and terminal zone of entangled polymer melts. The theory of the effect of chain-scission of polypropylene (and whether it occurs randomly) on molar mass has been described by Mead [78]. Simple mixing rules for the melt flow index and the steady-state recoverable compliance consistent with the double reptation model were also derived by Mead [78] to predict the effect of the reactive extrusion vis-breaking of polypropylene on the resulting linear viscoelastic material properties.

Viscoelastic measurements are a well-established and practical experimental method for melt characterization. The "inverse problem" of obtaining a MMD by analysis of linear viscoelastic behaviour has been the subject of many papers [79-89] since, in principle, rheological data is a powerful method for deriving the MMD of flexible polymers that is complementary or an alternative method to SEC and to polymers that are difficult to dissolve or insoluble in common solvents. The process used for obtaining the MMD and the molar mass averages from viscoelastic measurements is described in the following section.

3.4. Molar mass distributions from rheological properties

The rheological behaviour from the viscoelastic measurements of the virgin and controlled rheology samples has been analysed to obtain the MMD and the Mn, Mw and Mz molar mass averages. An inversion procedure for converting the linear viscoelastic data of polymer melts in terms of the storage (G′) and loss (G″) moduli into MMD was implemented in previous works by Nobile and Cocchini [84-86]. The problem was divided into two well-defined steps: the first was to define a direct relationship, based on physical concepts, which gives the rheological behaviour as a function of the MMD; the second consists in the use of a mathematical method to invert the above relationship.

In the direct way, a viscoelastic model [84, 86] was developed to calculate G′ and G″ from known MMD. It was based on the double reptation mixing rule [72-74, 76] and the MMD dependent kernel introduced by Thimm et al. [83, 90] correlating the relaxation time spectrum h(τ) to the MMD function *w(M)*

$$h\left[\tau\left(M\right)\right]=\tilde{h}\left(M\right)=G_N^0\left(\frac{2}{\alpha}\right)w\left(M\right)\left(\int_M^\infty\frac{w(M')}{M'}dM'\right) \qquad 6$$

where α ≈ 3.4 is the scaling exponent for the uniform case in the scaling relation for the relaxation time as a function of the molar mass *M* and
is the plateau modulus.

This relation was generalized by Nobile and Cocchini [86] to a Baumgaertel–Schausberger–Winter (BSW) form [91]; so the direct relationship developed in Nobile and Cocchini [86] was equation (7):

$$h\left(\tau\right)=n\tau^n\int_\tau^\infty\frac{\tilde{h}[M(\lambda)]}{\lambda^n}\frac{d\lambda}{\lambda} \qquad 7$$

with the scaling relation equation (8)

$$\lambda=\lambda\left(M\right)=k\frac{n+1}{n}M^\alpha \qquad 8$$

where n is the BSW parameter [91].

The model viscoelastic functions G′ and G″ can then be obtained from the relaxation time spectrum through well-known relationships [48] and are related to the MMD as shown in equation (9) and (10).

$$G'\left(\omega\right)=\int_0^\infty h\left(\tau\right)\frac{\left(\omega\tau\right)^2}{1+\left(\omega\tau\right)^2}\frac{d\tau}{\tau} \qquad 9$$

$$G''\left(\omega\right)=\int_0^\infty h(\tau)\frac{\omega\tau}{1+\left(\omega\tau\right)^2}\frac{d\tau}{\tau} \qquad 10$$

Regardless of the approach used to correlate the MMD to the rheological properties, the inversion of such relations is an ill-posed problem, as the MMD is very sensitive to small changes in the rheological measurements. The approaches used in literature rely on the use of some a priori knowledge of the behaviour of the MMD [79-89]. In particular, the three-parameter generalised exponential function (GEX) [92-93] is able to describe a wide class of uniform MMD in terms of three free parameters, a, b and M_0

$$w_{GEX}\left(a,b,M_0,M\right)=\frac{b}{\Gamma\left(\frac{a+1}{b}\right)}\left(\frac{M}{M_0}\right)^{a+1}\exp\left[-\left(\frac{M}{M_0}\right)^b\right] \qquad 11$$

This function gives rise to the meaningful triplets of the Mn, Mw, Mz averages

$$M_{\mathrm{n}}=M_0\frac{\Gamma\left(\frac{a+1}{b}\right)}{\Gamma\left(\frac{a}{b}\right)},\quad M_{\mathrm{w}}=M_0\frac{\Gamma\left(\frac{a+2}{b}\right)}{\Gamma\left(\frac{a+1}{b}\right)}\quad\text{and}\quad M_{\mathrm{z}}=M_0\frac{\Gamma\left(\frac{a+3}{b}\right)}{\Gamma\left(\frac{a+2}{b}\right)} \qquad 12$$

In this work, as in Nobile and Cocchini previous works [84-86] the *w*(M) in Equation (5) has been constrained to the GEX function. Therefore, the MMD function and the model rheological functions G'_{GEX} and G''_{GEX} are univocally identified by the three GEX parameters a, b and M_0. The inversion procedure consists in fitting the model viscoelastic functions G'_{GEX} and G''_{GEX} to the G'_j and G''_j (j = 1, 2, … N) raw data (Fig. 9; HP400N series) through a numerical minimization of the objective χ^2 function in terms of the three degrees of freedom

$$\chi^2(a,b,M_0) = \sum_{j=1}^{N} \left| \frac{G'_j - G'_{\mathrm{GEX}}(a,b,M_0,\omega_j)}{\varepsilon G'_j} \right|^2 + \sum_{j=1}^{N} \left| \frac{G''_j - G''_{\mathrm{GEX}}(a,b,M_0,\omega_j)}{\varepsilon G''_j} \right|^2 \qquad 13$$

where a constant relative error ε on the dynamic data is assumed.

Fig. 9

The MMD curves as well as the Mn, Mw and Mz averages for the virgin polypropylene samples have been obtained from the rheological G′ and G″ raw data, according to the described procedure. The MMD obtained from the inversion procedure applied to the G′ and G″ rheological data is shown in Fig. 10 for the HP400N together with the corresponding SEC results. The predictions based on rheological analysis closely match the MMD of the polypropylene obtained from SEC measurements. The molar mass averages are compared in Fig. 13. Similar findings were made for virgin HP555G (Fig. 14).

Fig. 10

Fig. 11

Fig. 12

Fig. 13

Fig. 14

In the case of the vis-broken samples, whose MMD curves shift from the original position towards lower molar mass, the lack of viscoelastic experimental data at high frequencies creates unacceptable uncertainty in the estimate of Mn from the rheological model. In this work, a further constraint has thus been introduced in the rheological model for the inversion of the G′ and G″ data of the controlled rheology polypropylene samples in order to obtain their MMD. In that the vis-breaking process preferentially cleaves chains of higher molar mass, a dramatic decrease is expected in Mz and Mw while only minor changes are expected to occur for in Mn. This approximation is also justified by the SEC analysis. Therefore the Mn value for each of the controlled rheology polypropylene samples has been constrained to the corresponding Mn value evaluated from the G′ and G″ data of the virgin sample. The procedure is developed in detail in Nobile et al. [94]. In Figs. 11 and 12, the MMD obtained from the inversion procedure (rheological GEX model) applied to rheological data of polymers of similar MFR formed by vis-breaking with aqueous peroxide and DHBP appear similar and compare well with the corresponding SEC results.

The results of the inversion procedure applied to the rheological data of both the HP400N and HP555G series in terms of the molar mass averages are reported in Fig. 13a and b respectively and compared with the corresponding averages from SEC analysis. The molar mass averages obtained from the rheological analysis for polymers of similar MFR formed by vis-breaking with aqueous peroxide and DHBP appear similar and are generally consistent with the corresponding results from SEC analysis.

Importantly, in the present context, the results confirm the close similarity of polypropylenes of the same or similar MFR obtained with hydrogen-peroxide-induced vis-breaking and DHBP-induced vis-breaking.

3.5. Crystallinity (WAXS, SAXS, DSC, density)

The crystallinity of the polypropylene as extruded was examined by differential scanning calorimetry (DSC) (1st heating), density measurements [46] and wide and small angle X-ray

diffraction (WAXS and SAXS). The data are presented in Table 1 (DSC, density for HP400N series), Table 2 (DSC, density for HP555G series), Table 3 (WAXS and SAXS for HP400N series) and Table 4 (WAXS and SAXS for HP555G series) and the fraction crystallinity obtained by the various methods is compared in Fig. 15. The methods (other than SAXS) provide a consistent value for the fraction crystallinity of the virgin polymer.

Table 3

Table 4

Fig. 15

Analysis of the WAXS (conventional X-ray source) (Fig. 13) indicates that the crystallinity of the vis-broken product is reduced from the precursor polypropylene (Table 3, Table 4). On the other hand, The DSC (1st heating) and density measurements suggest that the crystallinity, if anything, increases on scissioning (Table 1, Table 2). This apparent discrepancy prompted us to obtain further WAXS with much improved signal to noise using the Australian Synchrotron. However, the data obtained showed that the samples had changed over 2 years but nonetheless confirmed the earlier findings with respect to fraction crystallinity. SAXS were obtained simultaneously with WAXS in the synchrotron experiments. The fraction crystallinity suggested by the SAXS measurements is very different to that indicated by the other techniques for both virgin and scissioned polypropylene. This can be attributed to the different definition of fraction crystallinity inherent in SAXS analysis [95]. SAXS is sensitive to the amorphous component in between the crystalline lamellae, while the analysis of WAXS is sensitive to the overall fraction crystallinity.

The DSC (2nd heating) suggests that the crystallinity is the same for both virgin and scissioned samples, which suggests that any differences seen for the “as produced” samples reflect the history and differences in the morphology or spherulite size, rather than any intrinsic differences in the polypropylene. The results of CRYSTAF measurements (below) also support this hypothesis.

It is clear that crystallinity of the hydrogen peroxide-scissioned polypropylene and DHBP-scissioned polypropylene are similar regardless of the method by which it was determined.

3.6. Crystallizability (CRYSTAF)

Crystallization analysis fractionation (CRYSTAF) in which a solution of polypropylene is slowly cooled is a measure of the crystallizability of the polypropylene. This analysis showed no significant differences between the commercial polymer and the vis-broken polymer or between hydrogen peroxide- and DHBP-scissioned samples. The traces all exhibited a single sharp peak accounting for ~90–91% of the sample for HP400N and 91–92% for HP555G (Table 5). This peak is attributed to the crystallization of isotactic polypropylene. Six replicate runs were conducted for the two DHBP-scissioned samples which showed little variability in the fraction crystallized but some variation in the crystallization temperature.

Table 5

The controlled rheology polypropylenes are, however, very different from polypropylene produced in thermo-oxidative degradation [39]. The CRYSTAF trace is generally unaffected by changes in molar mass but is sensitive to changes in chemical composition or microstructure [96].

The CRYSTAF results are therefore qualitative evidence that there is no significant functionalization of the polypropylene backbone during the vis-breaking process with either

hydrogen peroxide or DHBP. Consistent with this, FTIR spectra of the vis-broken polypropylenes showed no spectral features consistent with oxidative scissioning (e.g., carbonyl absorptions).

4. Conclusions

Aqueous hydrogen peroxide has been shown to be an effective reagent for chain scissioning or vis-breaking polypropylene to produce a controlled rheology polymer in a melt extrusion process. The process produces a polypropylene with similar characteristics (molar mass, MMD, melt rheology, crystallinity) to that produced with an organic peroxide (DHBP) according to the conventional procedure, but the hydrogen peroxide-scissioned polypropylene has the distinct advantage that it contains no organic volatile contaminants attributable to use of a peroxide.

Acknowledgements

High temperature SEC and CRYSTAF measurements were performed by Robert Bruell, Fraunhofer for Structural Durability and System Reliability, Darmstadt.

References

[1] M. Xanthos, Process analysis from reaction fundamentals, M. Xanthos (Ed.), Reactive extrusion, Hanser, Munich (1992), pp. 33-55
[2] S.B. Brown, Reactive extrusion: a survey of chemical reactions of monomers and polymers during extrusion processing, M. Xanthos (Ed.), Reactive extrusion, Hanser, Munich (1992), pp. 75-199
[3] G. Moad, Prog Polym Sci, 24 (1999), pp. 81-142
[4] A.H. Hogt, J. Meijer, J. Jenenic, Modification of polypropylene by organic peroxides, S. Al-Malaika (Ed.), Reactive modifiers for polymers, Chapman & Hall, London (1997), pp. 84-132
[5] H. Azizi, I. Ghasemi, Polym Test, 23 (2) (2004), pp. 137-143
[6] H. Azizi, I. Ghasemi, Iran Polym J, 14 (5) (2005), pp. 465-471
[7] S.-H. Pong, C.-P. Lu, M.-C. Wang, S.-H.J. Chiu, Appl Polym Sci, 95 (2) (2005), pp. 280-289
[8] H. Azizi, I. Ghasemi, Q. Karrabi, Polym Test, 27 (5) (2008), pp. 548-554
[9] S. Echeverrigaray, R.D. Cruz, R.B. Oliveira, Polym Bull (2012), pp. 1-14
[10] P.A.R. Muñoz, S.H.P. Bettini, J Appl Polym Sci, 127 (1) (2013), pp. 87-95
[11] G.E. Garrett, E. Mueller, D.A. Pratt, J.S. Parent, Macromolecules, 47 (2) (2014), pp. 544-551
[12] N.M. Tollefson, S. Roy, T.A. Shepard, W.J. Long, Polym Eng Sci, 36 (1) (1996), pp. 117-125
[13] A. Pabedinskas, W.R. Cluett, S.T. Balke, Polym Eng Sci, 29 (15) (1989), pp. 993-1003
[14] C. Tzoganakis, Y. Tang, J. Vlachopoulos, A.E. Hamielec, Polym Plast Technol Eng, 28 (3) (1989), pp. 319-350
[15] S.H. Ryu, C.G. Gogos, M. Xanthos, Adv Polym Technol, 11 (2) (1991), pp. 121-131
[16] V.J. Triacca, P.E. Gloor, S. Zhu, A.N. Hrymak, A.E. Hamielec, Polym Eng Sci, 33 (8) (1993), pp. 445-454
[17] C. Tzoganakis, Can J Chem Eng, 72 (4) (1994), pp. 749-754
[18] M.J. Krell, A. Brandolin, E.M. Vallés, Polym React Eng, 2 (4) (1994), pp. 389-408
[19] F. Berzin, B. Vergnes, L. Delamare, J Appl Polym Sci, 80 (8) (2001), pp. 1243-1252
[20] A.V. Machado, J.M. Maia, S.V. Canevarolo, J.A. Covas, J Appl Polym Sci, 91 (4) (2004), pp. 2711-2720
[21] J.A. Oliveira, E.C. Biscaia, J.C. Fadigas, J.C. Pinto, Macromol Mater Eng, 291 (5) (2006), pp. 552-570
[22] B. Kalantari, R. Semnani Rahbar, M.R.M. Mojtahedi, S.A. Mousavi Shoushtari, A. Khosroshahi, J Appl Polym Sci, 105 (4) (2007), pp. 2287-2293
[23] K. Sirin, M. Yavuz, M. Çanli, A. Avci, F. Dogan, J Polym Mater, 30 (4) (2013), pp. 381-396
[24] M.J. Scorah, S. Zhu, A. Psarreas, N.T. McManus, R. Dhib, C. Tzoganakis, et al., Polym Eng Sci, 49 (9) (2009), pp. 1760-1766
[25] C. Tzoganakis, J. Vlachopoulos, A.E. Hamielec, Polym Eng Sci, 28 (3) (1988), pp. 170-180

[26] P.D. Iedema, C. Willems, G. van Vliet, W. Bunge, S.M.P. Mutsers, H.C.J. Hoefsloot, Chem Eng Sci, 56 (12) (2001), pp. 3659-3669
[27] M. Zummallen, Controlled-rheology polypropylene, method of preparation and article, Dow Global Technologies Inc., USA (2010) US20100324225A1
[28] M. Aubert, M. Roth, R. Pfaendner, C.-E. Wilén, Macromol Mater Eng, 292 (6) (2007), pp. 707-714
[29] R. Pfaendner, C. R. Chim, 9 (11–12) (2006), pp. 1338-1344
[30] A. Psarreas, C. Tzoganakis, N. McManus, A. Penlidis, Polym Eng Sci, 47 (12) (2007), pp. 2118-2123
[31] A. Schneider, M. Roth, Chem Fibers Int, 56 (2006), pp. 177-179
[32] G. He, C. Tzoganakis, Polym Eng Sci, 51 (1) (2011), pp. 151-157
[33] D. Tripathi, Practical guide to polypropylene, iSmithers Rapra Publishing, Shrewsbury, UK (2002), p. p 11
[34] I.J. Dagley, G. Moad, L.V. Nichols, Modification of propylene polymers, Polymers CRC (2012)
[35] W. Zhou, S. Zhu, Ind Eng Chem Res, 36 (4) (1997), pp. 1130-1135
[36] D. Bertin, S. Grimaldi, M. Leblanc, S.R.A. Marque, D. Siri, P. Tordo, J Mol Struct Theochem, 811 (1–3) (2007), pp. 255-266
[37] D. Bertin, M. Leblanc, S.R.A. Marque, D. Siri, Polym Degr Stab, 95 (5) (2010), pp. 782-791
[38] G. Gryn'ova, J.L. Hodgson, M.L. Coote, Org Biomol Chem, 9 (2) (2011), pp. 480-490
[39] S. de Goede, R. Brüll, H. Pasch, N. Marshall, Macromol Symp, 193 (1) (2003), pp. 35-44
[40] P. Dokolas, S.M. Loer, D.H. Solomon, Aust J Chem, 51 (12) (1998), pp. 1113-1120
[41] S. Camara, B.C. Gilbert, R.J. Meier, M. van Duin, A.C. Whitwood, Org Biomol Chem, 1 (7) (2003), pp. 1181-1190
[42] P.A. Giguère, I.D. Liu, Can J Chem, 35 (4) (1957), pp. 283-293
[43] J. Troe, Combust Flame, 158 (4) (2011), pp. 594-601
[44] G. Moad, M.S. O'Shea, G. Peeters, A. Postma, Modification of polyolefins, Advanced Polymerik (2009)
[45] ASTM standard E313-10 standard practice for calculating yellowness and whiteness indices from instrumentally measured color coordinates, ASTM International, West Conshohocken, PA (2010)
[46] J.R. Isasi, L. Mandelkern, M.J. Galante, R.G. Alamo, J Polym Sci B Polym Phys, 37 (4) (1999), pp. 323-334
[47] P.-W. Zhu, J. Tung, A. Phillips, G. Edward, Macromolecules, 39 (5) (2006), pp. 1821-1831
[48], J.D. Ferry, Viscoelastic properties of polymers, (3rd ed.), Wiley, New York (1980), pp. 264-320,
[49] D.S. Pearson, L.J. Fetters, L.B. Younghouse, J.W. Mays, Macromolecules, 21 (2) (1988), pp. 478-484
[50] H. Mavridis, R.N. Shroff, Polym Eng Sci, 32 (23) (1992), pp. 1778-1791
[51] A. Eckstein, C. Friedrich, A. Lobbrecht, R. Spitz, R. Mulhaupt, Acta Polym, 48 (1–2) (1997), pp. 41-46
[52] A. Eckstein, J. Suhm, C. Friedrich, R.D. Maier, J. Sassmannshausen, M. Bochmann, et al., Macromolecules, 31 (4) (1998), pp. 1335-1340
[53] S.H. Wasserman, W.W. Graessley, Polym Eng Sci, 36 (6) (1996), pp. 852-861
[54] K. Bernreitner, W. Neissl, M. Gahleitner, Polym Test, 11 (2) (1992), pp. 89-100
[55] C. Tzoganakis, J. Vlachopoulos, A.E. Hamielec, D.M. Shinozaki, Polym Eng Sci, 29 (6) (1989), pp. 390-396
[56] G. Barakos, E. Mitsoulis, C. Tzoganakis, T. Kajiwara, J Appl Polym Sci, 59 (3) (1996), pp. 543-556
[57] K. Yasuda, R.C. Armstrong, R.E. Cohen, Rheol Acta, 20 (2) (1981), pp. 163-178
[58] R.P. Wool, Macromolecules, 26 (7) (1993), pp. 1564-1569
[59] G. Petragli, A. Coen, Polym Eng Sci, 10 (2) (1970), p. 79

[60] D.L. Plazek, D.J. Plazek, Macromolecules, 16 (9) (1983), pp. 1469-1475
[61] G.R. Zeichner, P.D. Patel, Proc 2nd world congr chem eng Montreal (1981), pp. 6-9
[62] C. Carrot, P. Revenu, J. Guillet, J Appl Polym Sci, 61 (11) (1996), pp. 1887-1897
[63] W. Minoshima, J.L. White, J.E. Spruiell, Polym Eng Sci, 20 (17) (1980), pp. 1166-1176
[64] M. Aguilar, J.F. Vega, B. Pena, J. Martinez-Salazar, Polymer, 44 (5) (2003), pp. 1401-1407
[65] M. Fujiyama, H. Inata, J Appl Polym Sci, 84 (12) (2002), pp. 2157-2170
[66] M.J. Struglinski, W.W. Graessley, Macromolecules, 18 (12) (1985), pp. 2630-2643
[67] S.H. Wasserman, W.W. Graessley, J Rheol, 36 (4) (1992), pp. 543-572
[68] B.H. Bersted, J Appl Polym Sci, 19 (8) (1975), pp. 2167-2177
[69] A.Y. Malkin, N.K. Blinova, Gv Vinograd, M.P. Zabugina, O.Y. Sabsai, Vc Shalgano, et al., Eur Polym J, 10 (5) (1974), pp. 445-451
[70] W.W. Graessley, M.J. Struglinski, Macromolecules, 19 (6) (1986), pp. 1754-1760
[71] M. Rubinstein, R.H. Colby, J Chem Phys, 89 (8) (1988), pp. 5291-5306
[72] C. Tsenoglou, Polym Prepr Am Chem Soc Div Polym Chem, 28 (2) (1987), pp. 185-186
[73] J. Descloizeaux, Europhys Lett, 5 (5) (1988), pp. 437-442
[74] J. Descloizeaux, Macromolecules, 23 (17) (1990), pp. 3992-4006
[75] D. Maier, A. Eckstein, C. Friedrich, J. Honerkamp, J Rheol, 42 (5) (1998), pp. 1153-1173
[76] C. Tsenoglou, Macromolecules, 24 (8) (1991), pp. 1762-1767
[77] P. Cassagnau, J.P. Montfort, G. Marin, P. Monge, Rheol Acta, 32 (2) (1993), pp. 156-167
[78] D.W. Mead, J Appl Polym Sci, 57 (2) (1995), pp. 151-173
[79] W.H. Tuminello, Polym Eng Sci, 26 (19) (1986), pp. 1339-1347
[80] D.W. Mead, J Rheol, 38 (6) (1994), pp. 1797-1827
[81] S.H. Wasserman, J Rheol, 39 (3) (1995), pp. 601-625
[82] C. Carrot, J. Guillet, J Rheol, 41 (5) (1997), pp. 1203-1220
[83] W. Thimm, C. Friedrich, T. Roths, J. Honerkamp, J Rheol, 44 (6) (2000), pp. 1353-1361
[84] F. Cocchini, M.R. Nobile, Rheol Acta, 42 (3) (2003), pp. 232-242
[85] M.R. Nobile, F. Cocchini, Rheol Acta, 40 (2) (2001), pp. 111-119
[86] M.R. Nobile, F. Cocchini, Rheol Acta, 47 (5–6) (2008), pp. 509-519
[87] F. Leonardi, A. Allal, G. Marin, J Rheol, 46 (1) (2002), pp. 209-224
[88] E. Van Ruymbeke, R. Keunings, C. Bailly, J Newt Fluid, 105 (2–3) (2002), pp. 153-175
[89] J.D. Guzman, J.D. Schieber, R. Pollard, Rheol Acta, 44 (4) (2005), pp. 342-351
[90] W. Thimm, C. Friedrich, M. Marth, J. Honerkamp, J Rheol, 43 (6) (1999), pp. 1663-1672
[91] M. Baumgaertel, A. Schausberger, H.H. Winter, Rheol Acta, 29 (5) (1990), pp. 400-408
[92] W.E. Gloor, J Appl Polym Sci, 22 (5) (1978), pp. 1177-1182
[93] W.E. Gloor, J Appl Polym Sci, 28 (2) (1983), pp. 795-805
[94] Nobile MR, Cocchini F, Dagley IJ, Habsuda J, Li G, Moad G, et al., 2015. To be submitted
[95] S. Rabiej, A. Wlochowicz, Angew Makromol Chem, 175 (1) (1990), pp. 81-97
[96] S. Anantawaraskul, J.P. Soares, P. Wood-Adams, Adv Polym Sci, 182 (2005), pp. 1-54

Table 1

Table 1. Properties of virgin and chain-scissioned polypropylene HP400N.

Material	Fraction crystallinity from DSC		T_m (°C) (1st heating)	T_c(°C)	Density (g cm^{-3})	Fraction crystallinity from density
	1st Heating	2nd Heating				
HP400N MFR 11	0.47	0.49	165.2	105.3	0.8893	0.453 ± 0.0012
H_2O_2 scissioned MFR 44.6	0.45	0.49	164.3	106.5	0.8892	0.452 ± 0.0009
DHBP scissioned MFR 44	0.48	0.49	164.4	106.6	0.8931	0.499 ± 0.0026
H_2O_2 scissioned MFR 77	0.51	0.50	165.6	106.7	0.8915	0.480 ± 0.0008

Table 2

Table 2. Properties of virgin and chain-scissioned polypropylene HP555G.

Material	Fraction crystallinity from DSC		T_m (°C) (1st heating)	T_c(°C)	Density (g cm^{-3})	Fraction crystallinity from density
	1st Heating	2nd Heating				
HP555G MFR 1.5	0.43	0.48	165.6	103.0	0.8900	0.461 ± 0.0016
H_2O_2 scissioned MFR 7.4	0.44	0.50	165.1	108.2	0.8930	0.498 ± 0.0011
DHBP scissioned MFR 9.8	0.45	0.49	164.8	106.3	0.8912	0.476 ± 0.0010
H_2O_2 scissioned MFR 24.0	0.48	0.51	164.9	108.8	0.8910	0.474 ± 0.0015

Table 3

Table 3. X-ray diffraction properties of virgin and chain-scissioned polypropylene HP400N.

Material	Conventional WAXS[a]	Fraction crystallinity		Synchrotron SAXS
		Conventional WAXS[b]	Synchrotron WAXS[b]	
HP400N MFR 11	0.47 ± 0.002	0.45	0.45	0.75
H_2O_2 scissioned MFR 44.6	0.39 ± 0.001	0.38	0.39	0.82
DHBP scissioned MFR 44	0.40 ± 0.002	0.38	0.41	0.74
H_2O_2 scissioned MFR 77	0.38 ± 0.002	0.36	0.35	0.77

a
Data processed using Traces® v6 (GBC Scientific Equipment, Hampshire, IL). Error bars indicate the reproducibility of the determination.

b
Data processed with Origin v8 (OriginLab, Northampton, MA).

Table 4

Table 4. X-ray diffraction properties of virgin and chain-scissioned polypropylene HP555G.

Material	Conventional WAXS[a]	Fraction crystallinity		Synchrotron SAXS
		Conventional WAXS[b]	Synchrotron WAXS[b]	
HP400N MFR 11	0.45 ± 0.001	0.43	0.43	0.81
H_2O_2 scissioned MFR 44.6	0.40 ± 0.002	0.39	0.37	0.80
DHBP scissioned MFR 44	0.40 ± 0.002	0.38	0.42	0.81
H_2O_2 scissioned MFR 77	0.35 ± 0.001	0.38	0.40	0.79

a
Data processed using Traces® v6 (GBC Scientific Equipment, Hampshire, IL). Error bars indicate the reproducibility of the determination.

b
Data processed with Origin v8 (OriginLab, Northampton, MA).

Table 5

Table 5. CRYSTAF data for HP400N, HP555G and scissioned samples.

Sample	Peak temperature (° C)	Fraction
HP400N MFR 11	78.4	0.909
H_2O_2 scissioned MFR 44.6	78.2	0.901
DHBP scissioned MFR 44	74.8±2[a]	0.912±1[a]
H_2O_2 scissioned MFR 77	78.6	0.898
HP555G MFR 1.5	78.3	0.921
H_2O_2 Scissioned MFR 7.4	68.4	0.926
DHBP Scissioned MFR 9.8	74.4±2[a]	0.911±1[a]
H_2O_2 Scissioned MFR 24.0	72.5	0.921

a
Average over two determinations.

Scheme 1

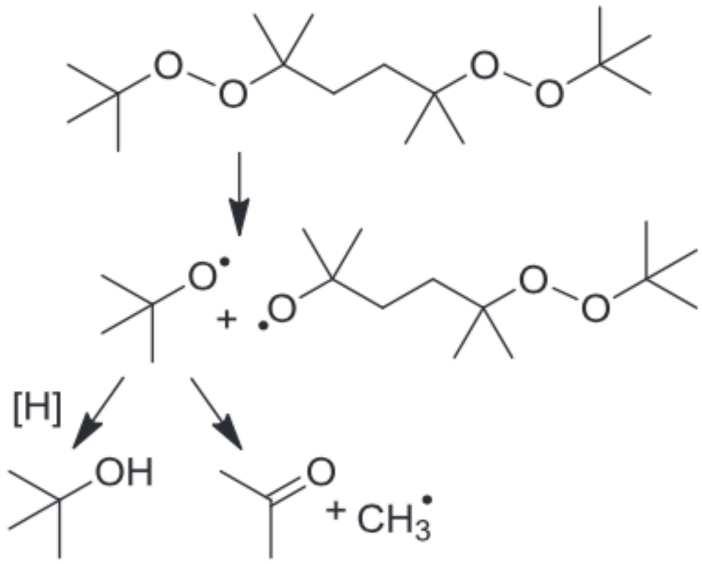

Scheme 1. Mechanism of thermal decomposition of 2,5-dimethyl-2,5-di-tert-butylperoxyhexane (DHBP). [H] is a hydrogen atom source, e.g., polypropylene.

Scheme 2.

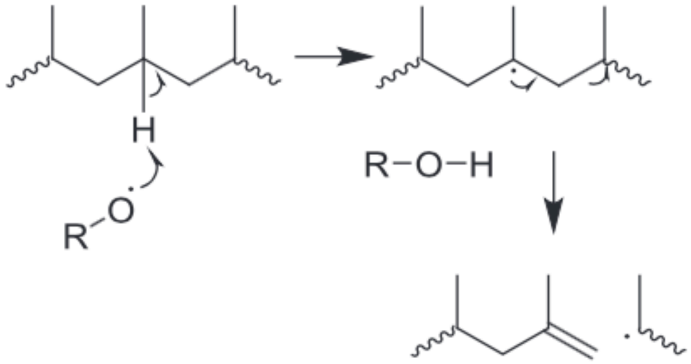

Scheme 2. Proposed mechanism of chain scission.

Fig. 1

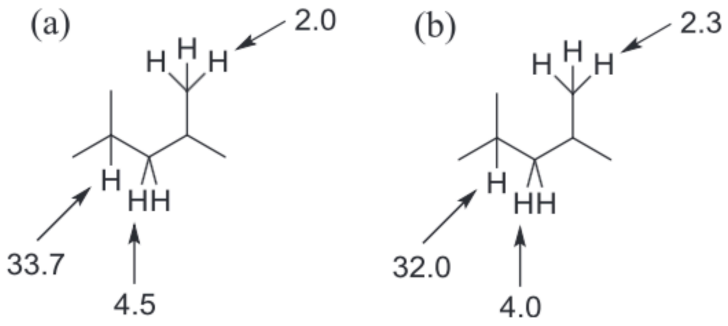

Fig. 1. Experimentally determined relative reactivity per hydrogen atom in abstraction by (a) cumyloxy radicals at 160 °C [11] (b) tert-butoxy radicals at 60 °C [40].

Fig. 2

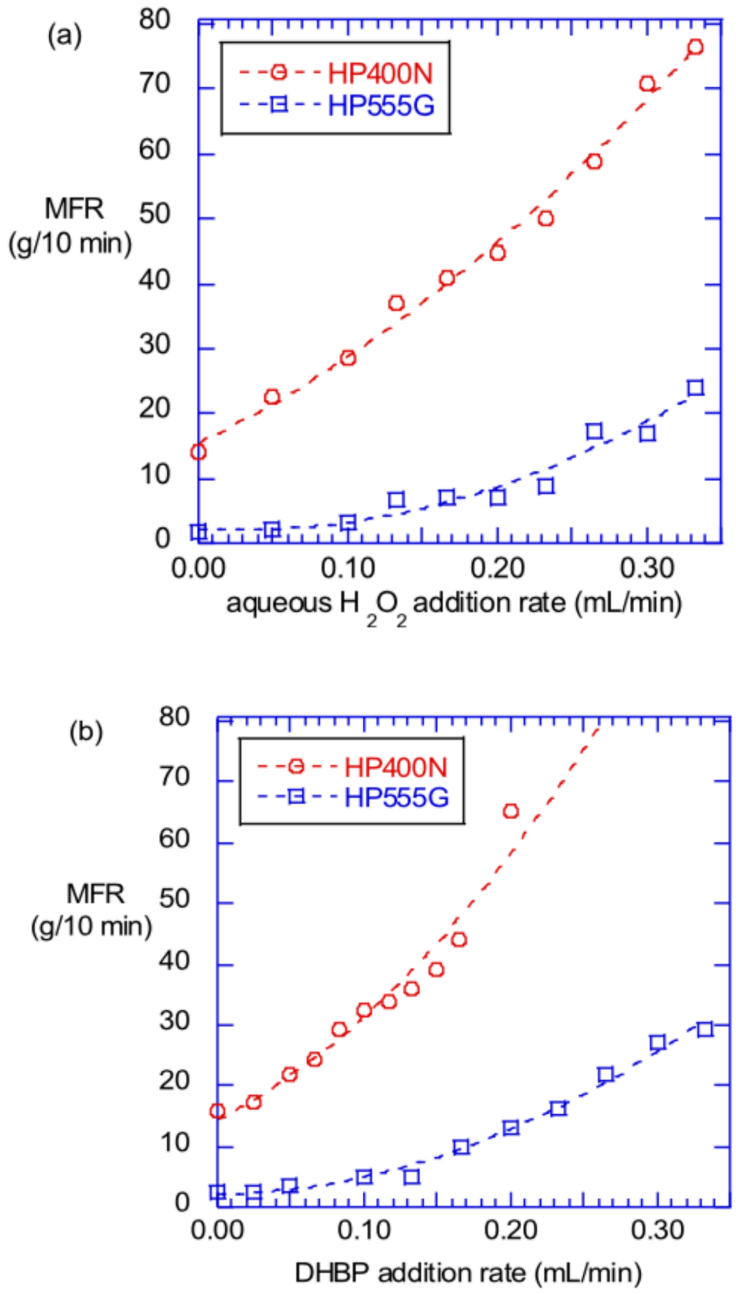

Fig. 2. Dependence of the extent of vis-breaking on peroxide addition rate for commercial polypropylenes (HP555G or HP400N) with (a) 60 %w/w aqueous hydrogen peroxide or (b) 2,5-dimethyl-2,5-di-tert-butylperoxyhexane (DHBP).

Fig. 3

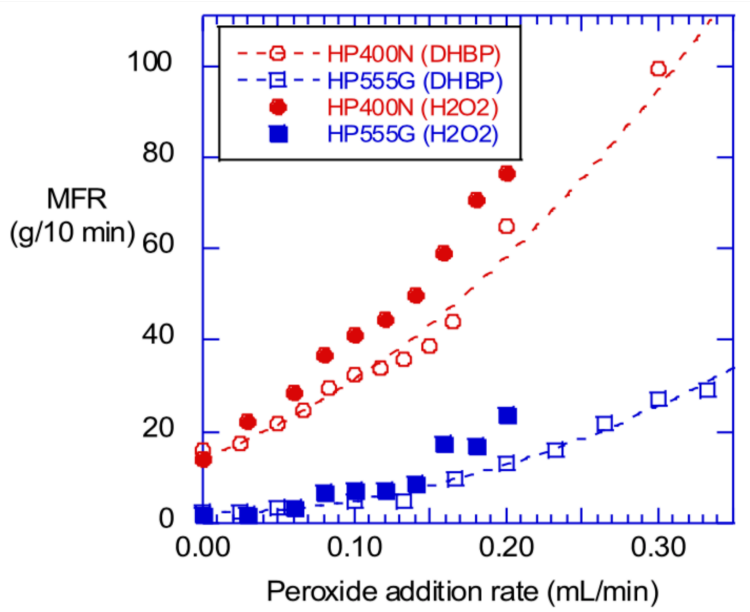

Fig. 3. Comparison of the dependence of vis-breaking of commercial polypropylenes on peroxide addition rate for hydrogen peroxide (corrected for concentration) and 2,5-dimethyl-2,5-di-tert-butylperoxyhexane (DHBP).

Fig. 4

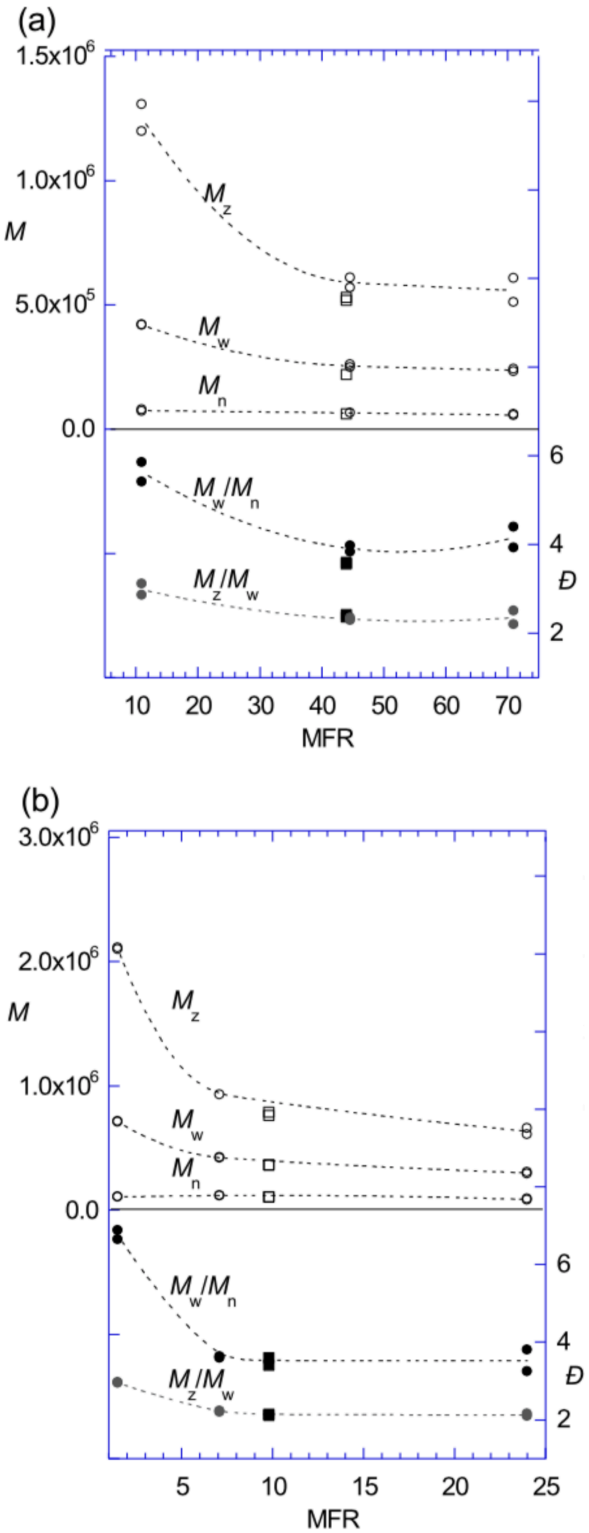

Fig. 4. Effect of vis-breaking with hydrogen peroxide (□) or 2,5-dimethyl-2,5-di-tert-butylperoxyhexane (DHBP) (○) on molar mass averages (in polystyrene equivalents) and dispersities for (a) polypropylene HP400N and (b) HP555G. The dotted lines are lines of best fit though the hydrogen peroxide data. Multiple data points indicate replicate experiments.

Fig. 5

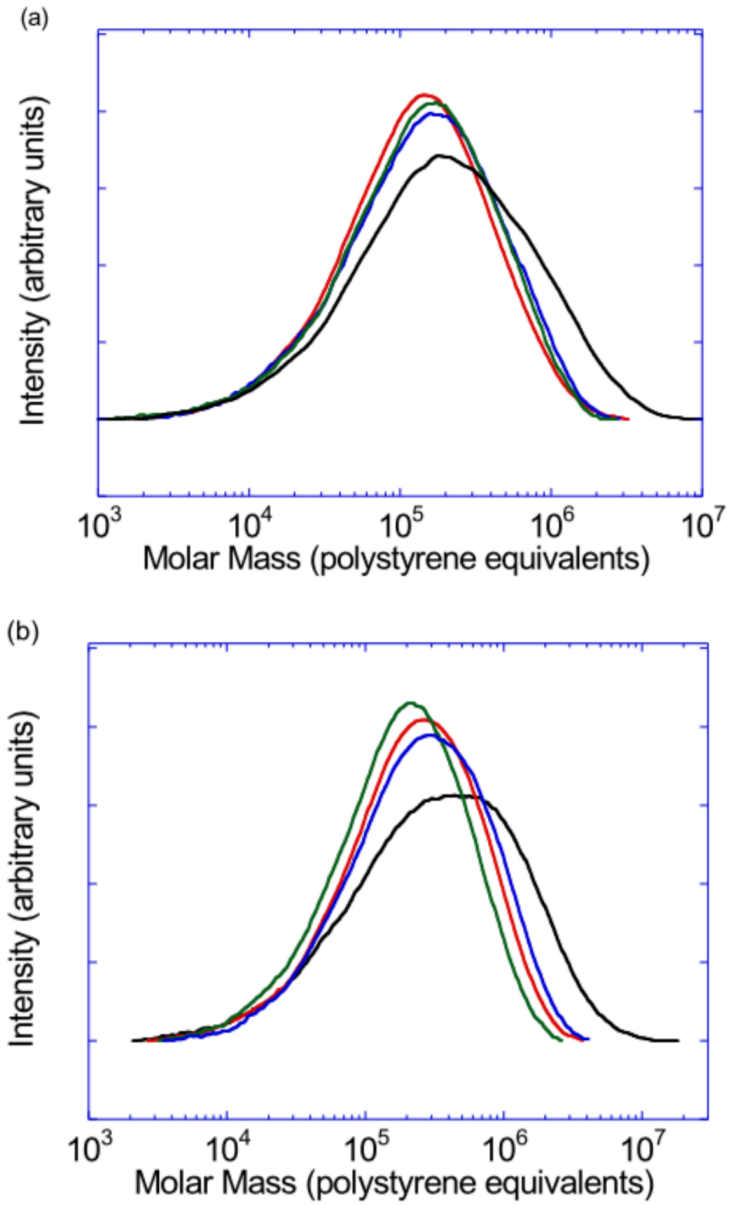

Fig. 5. Effect of vis-breaking with hydrogen peroxide or 2,5-dimethyl-2,5-di-tert-butylperoxyhexane (DHBP) on molar mass distributions (MMD) for polypropylene (a) HP400N: virgin polymer (——), H_2O_2-scissioned MFR 44.6 (——), H_2O_2-scissioned MFR 77 (——), DHBP-scissioned MFR 44 (——) and (b) HP555G: virgin polymer (——), H_2O_2-scissioned MFR 7.1 (——), H_2O_2-scissioned MFR 24 (——), DHBP-scissioned MFR 9.8 (——).

Fig. 6

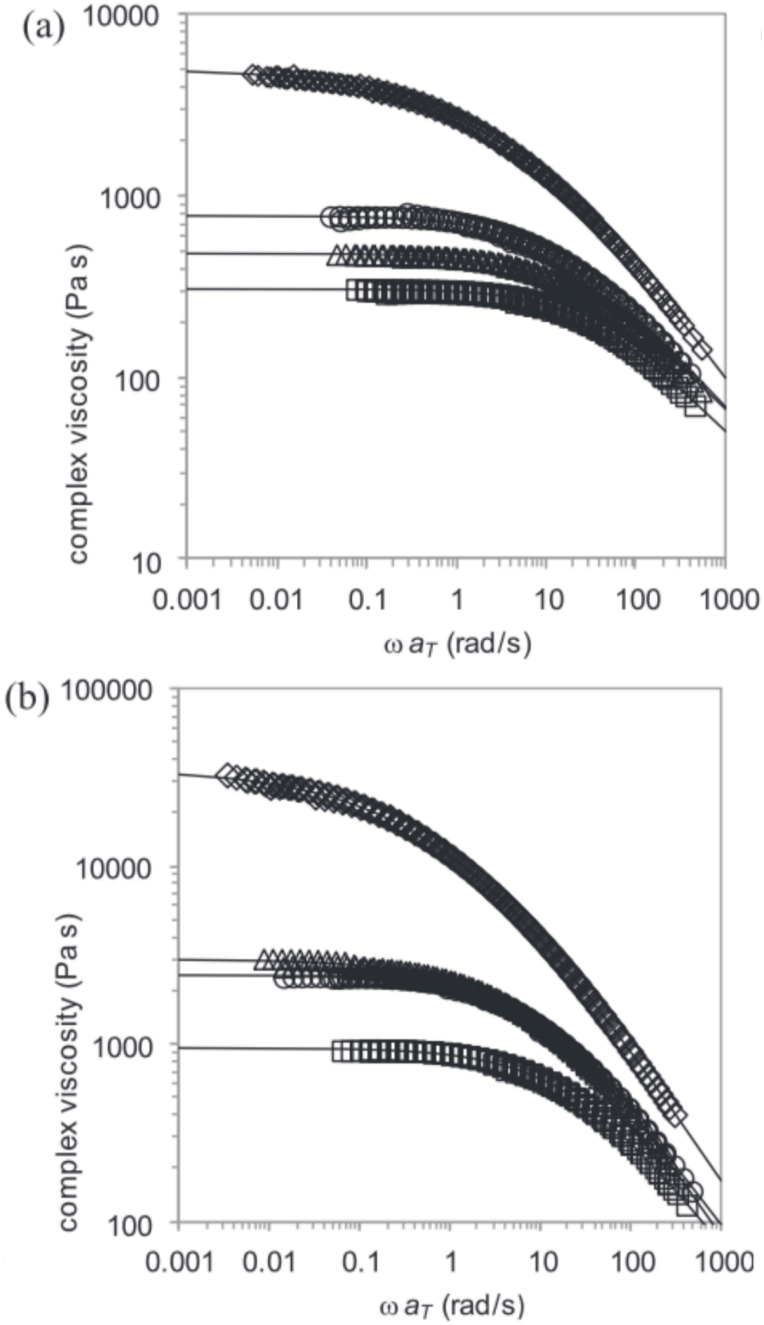

Fig. 6. Master curves of the complex viscosity for virgin polypropylene and the vis-broken samples derived from (a) HP400N and (b) HP555G series for the reference temperature (T0) of 190 °C. The continuous lines correspond to the Carreau–Yasuda model (equation (4)) fit to the complex viscosity data. The data points correspond to ◊ virgin polymer, Δ scissioned with 0.2 mL min^{-1} (~600 ppm) H_2O_2, ○ scissioned with 0.165 mL min^{-1} 2,5-dimethyl-2,5-di-tert-butylperoxyhexane (DHBP), □ scissioned with 0.33 mL min^{-1} (~1000 ppm) H_2O_2.

Fig. 7

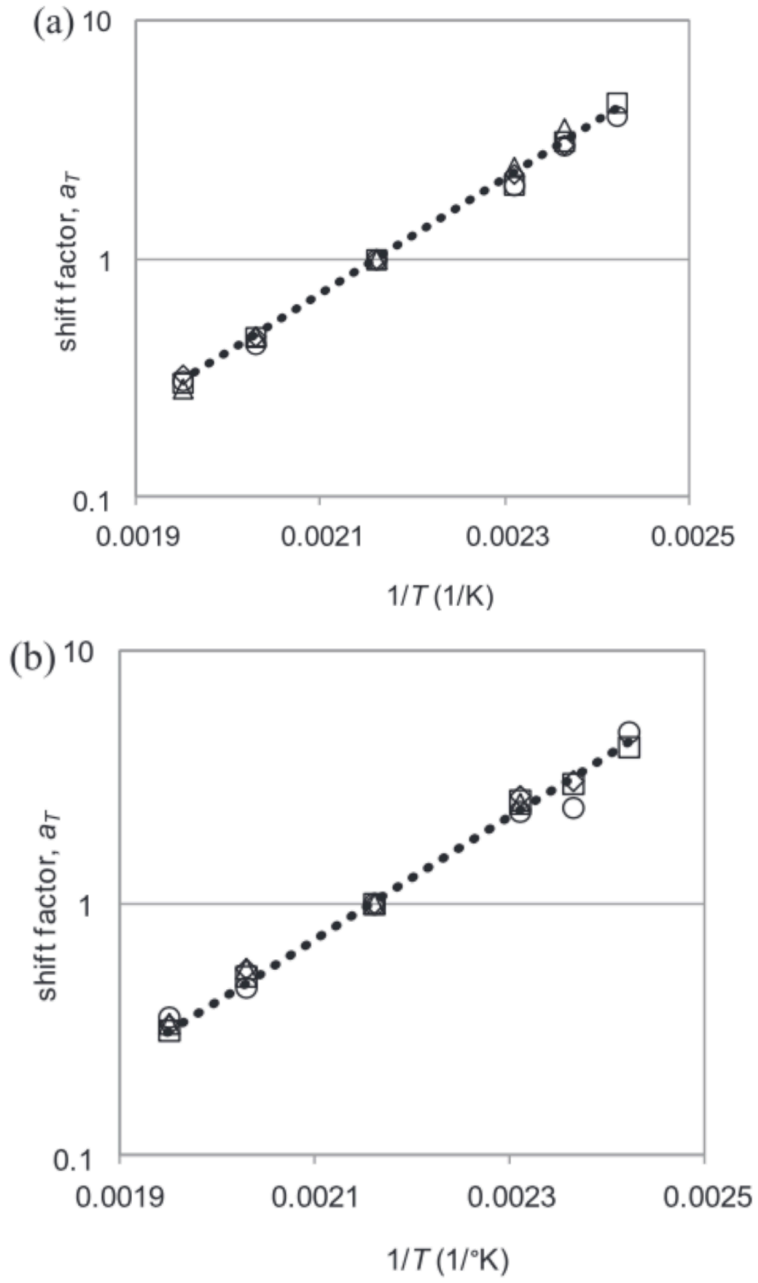

Fig. 7. Temperature dependence of the horizontal shift factors for a reference temperature T0 of 190 °C for (a) the HP400N series and (b) HP555G series. The dotted lines correspond to the Arrhenius equation with activation energies for flow Ea of 46.0 kJ mol−1 and 46.4 kJ mol−1 respectively. The data points correspond to ◊ virgin polymer, Δ scissioned with 0.2 mL min−1 (~600 ppm) H_2O_2, ○ scissioned with 0.165 mL min−1 2,5-dimethyl-2,5-di-tert-butylperoxyhexane (DHBP), □ scissioned with 0.33 mL min−1 (~1000 ppm) H_2O_2.

Fig. 8

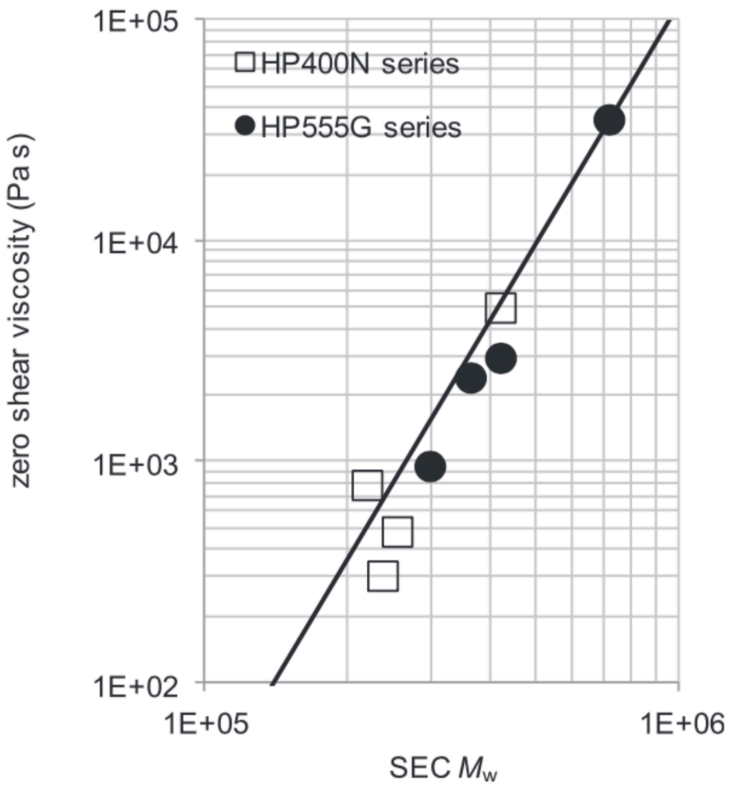

Fig. 8. Plot of the zero-shear viscosity (evaluated from the fit of complex viscosity data to the Carreau–Yasuda model) as a function of the weight average molar mass Mw (as obtained from SEC measurements) for the HP400N and the HP555G series of samples.

Fig. 9

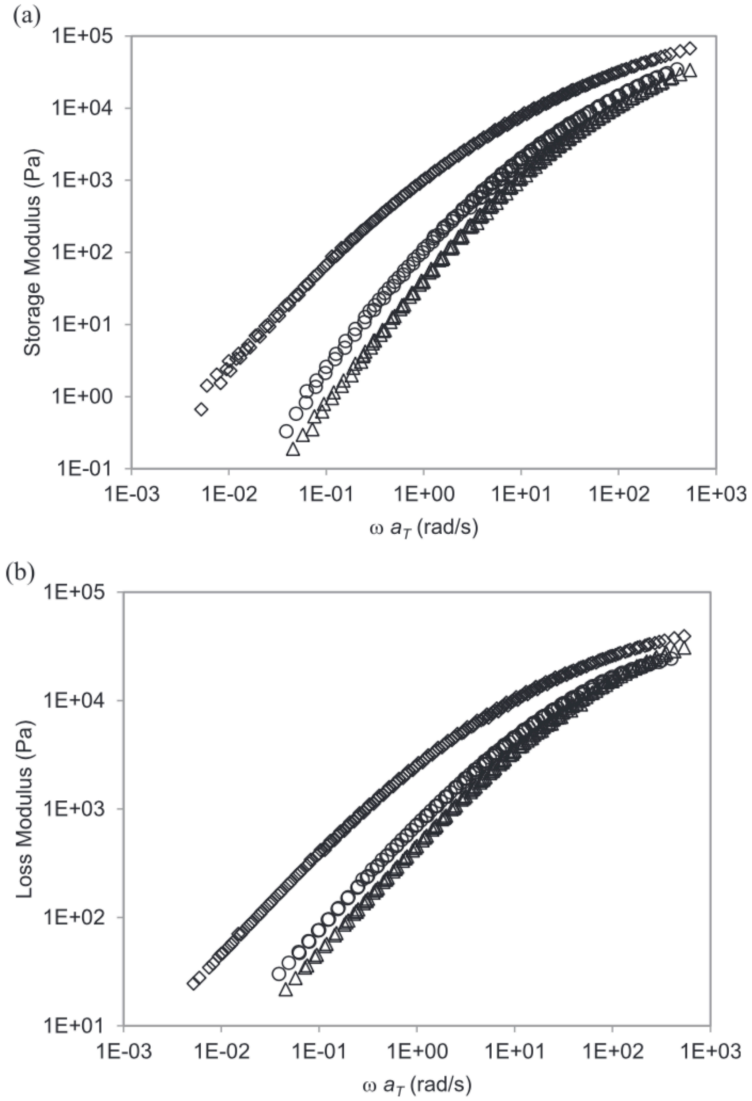

Fig. 9. Master curves of (a) the storage modulus,G′, and (b) loss modulus, G″ for the HP400N series. Reference temperature, T0 = 190 °C. The data points are ◊ virgin polymer, Δ scissioned with 0.2 mL min^{-1} (~600 ppm) H_2O_2, ○ scissioned with 0.165 mL min^{-1} 2,5-dimethyl-2,5-di-tert-butylperoxyhexane (DHBP).

Fig. 10

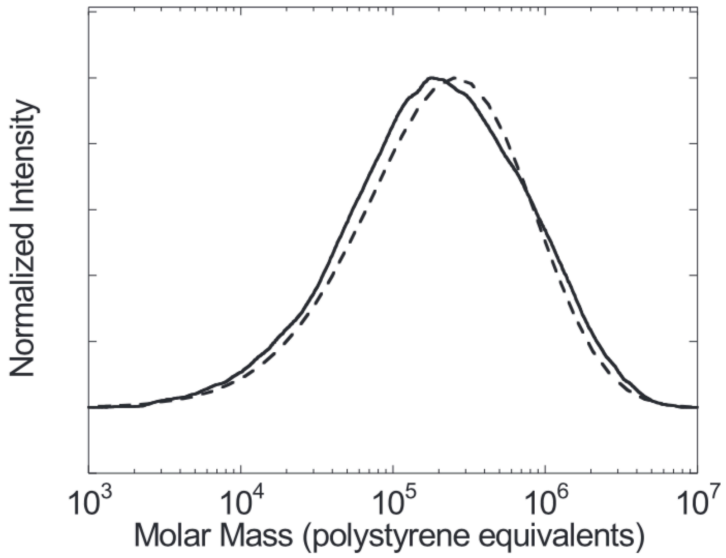

Fig. 10. Comparison of the SEC molar mass distributions (MMD) obtained directly from SEC analysis (—) and from application of the rheological GEX model (— — —) for virgin HP400N polypropylene.

Fig. 11

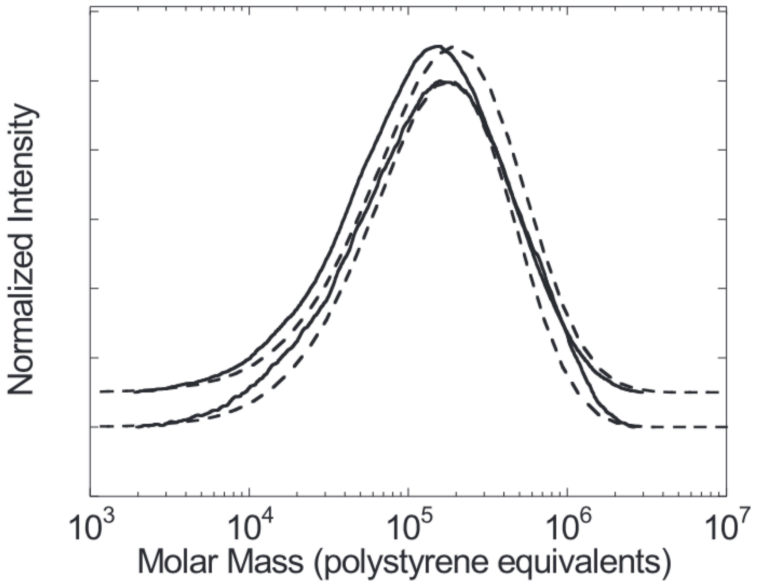

Fig. 11. Comparison of the SEC molar mass distributions (MMD) obtained directly from SEC analysis (—) and from application of the rheological GEX model (– – –) for HP400N polypropylene vis-broken with aqueous hydrogen peroxide to give MFR 44.6 (lower traces) and with 2,5-dimethyl-2,5-di-tert-butylperoxyhexane (DHBP) to give MFR 44.0 (upper traces).

Fig. 12

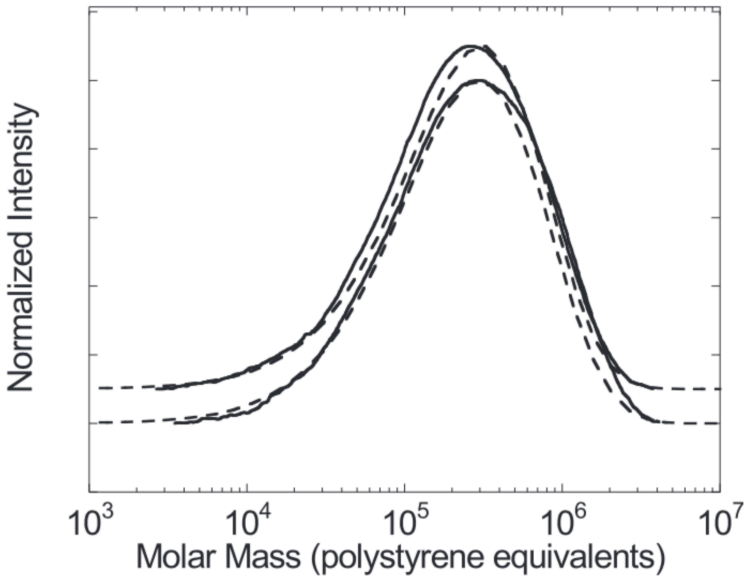

Fig. 12. Comparison of the SEC molar mass distributions (MMD) obtained directly from SEC analysis (—) and from application of the rheological GEX model (– – –) for HP555G polypropylene vis-broken with aqueous hydrogen peroxide to give MFR 7.1 (lower traces) and with 2,5-dimethyl-2,5-di-tert-butylperoxyhexane (DHBP) to give MFR 9.8 (upper traces).

Fig. 13

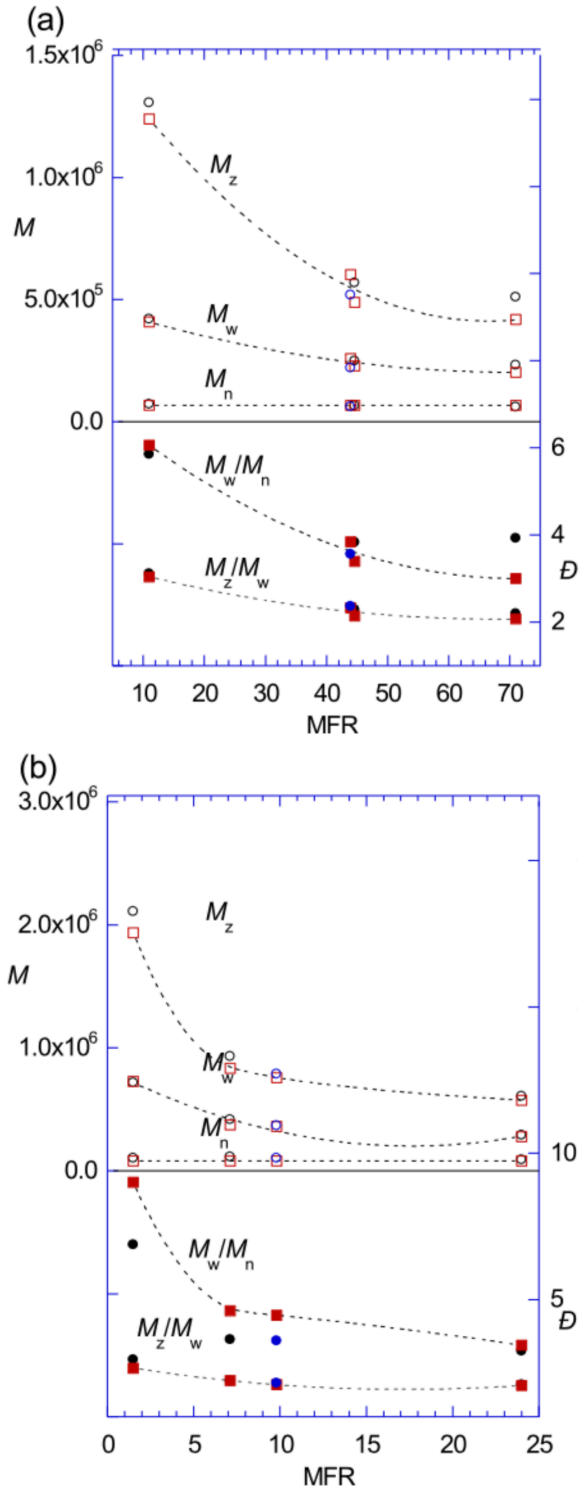

Fig. 13. Comparison of molar mass averages and dispersities obtained by fitting the rheological data to the GEX MMD model with "constrained Mn" [94] for the vis-broken samples (squares) and evaluated SEC measurements (circles, average of 2 measurements; refer Fig. 4) for (a) the HP400N series and (b) the HP555G series. Lines are lines of best fit through the rheological data. Note that in the analysis of the rheological data, the Mn values were constrained to a fixed value (see text).

Fig. 14

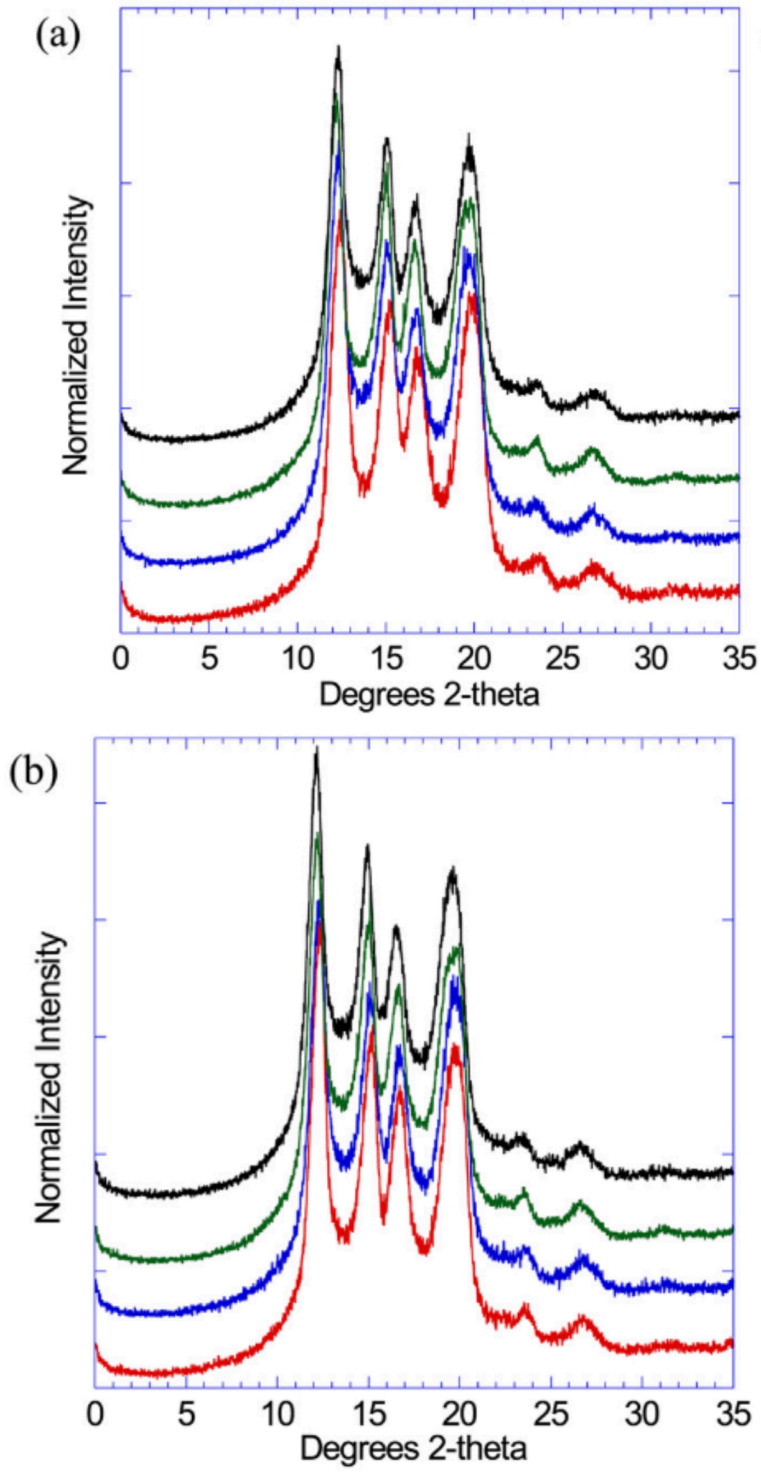

Fig. 14. Comparison of wide angle X-ray (WAXS – conventional X-ray source) for (a) the HP400N series and (b) the HP555G series. From bottom to top are shown the virgin polymer, scissioned with 0.2 mL min^{-1} (~600 ppm) H_2O_2, scissioned with 0.165 mL min^{-1} 2,5-dimethyl-2,5-di-tert-butylperoxyhexane (DHBP) and scissioned with 0.33 mL min^{-1} (~1000 ppm) H_2O_2.

Fig. 15

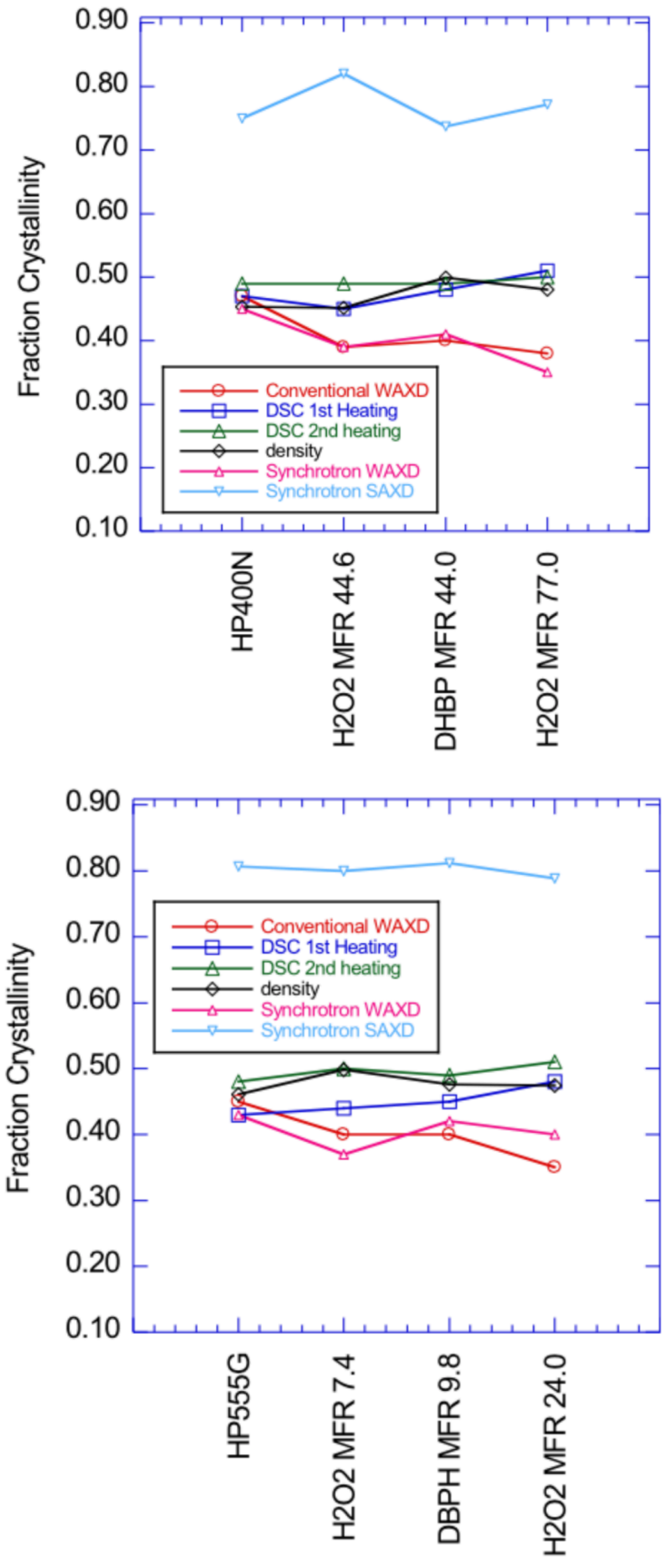

Fig. 15. Dependence of fraction crystallinity on vis-breaking.